Supplementary Information for "Quantifying the potential future contribution to global mean sea level from the Filchner-Ronne basin, Antarctica"

Emily A. Hill[1,2], Sebastian H. R. Rosier[2], G. Hilmar Gudmundsson[2], and Matthew Collins[1]

[1]College of Engineering, Mathematics and Physical Sciences, University of Exeter, Exeter, United Kingdom
[2]Department of Geography and Environmental Sciences, University of Northumbria, Newcastle-upon-Tyne, United Kingdom

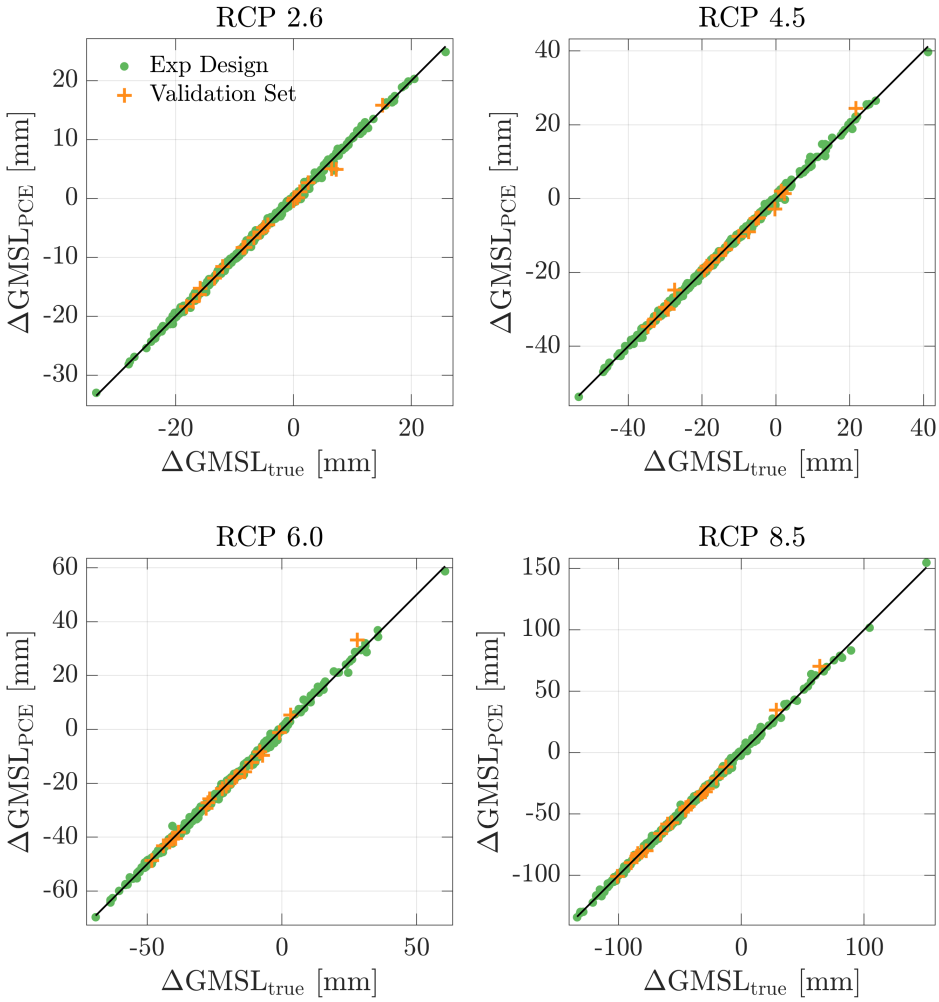

Figure S1. Performance of our surrogate (PCE) models ($\Delta\mathrm{GMSL}_{\mathrm{PCE}}$) with respect to our ice-flow model ($\Delta\mathrm{GMSL}_{\mathrm{true}}$) for each RCP scenario. Green points are from our 500 model ensemble that was used as a training set to create the PCE models. Orange crosses are an independent validation set of 20 model runs.

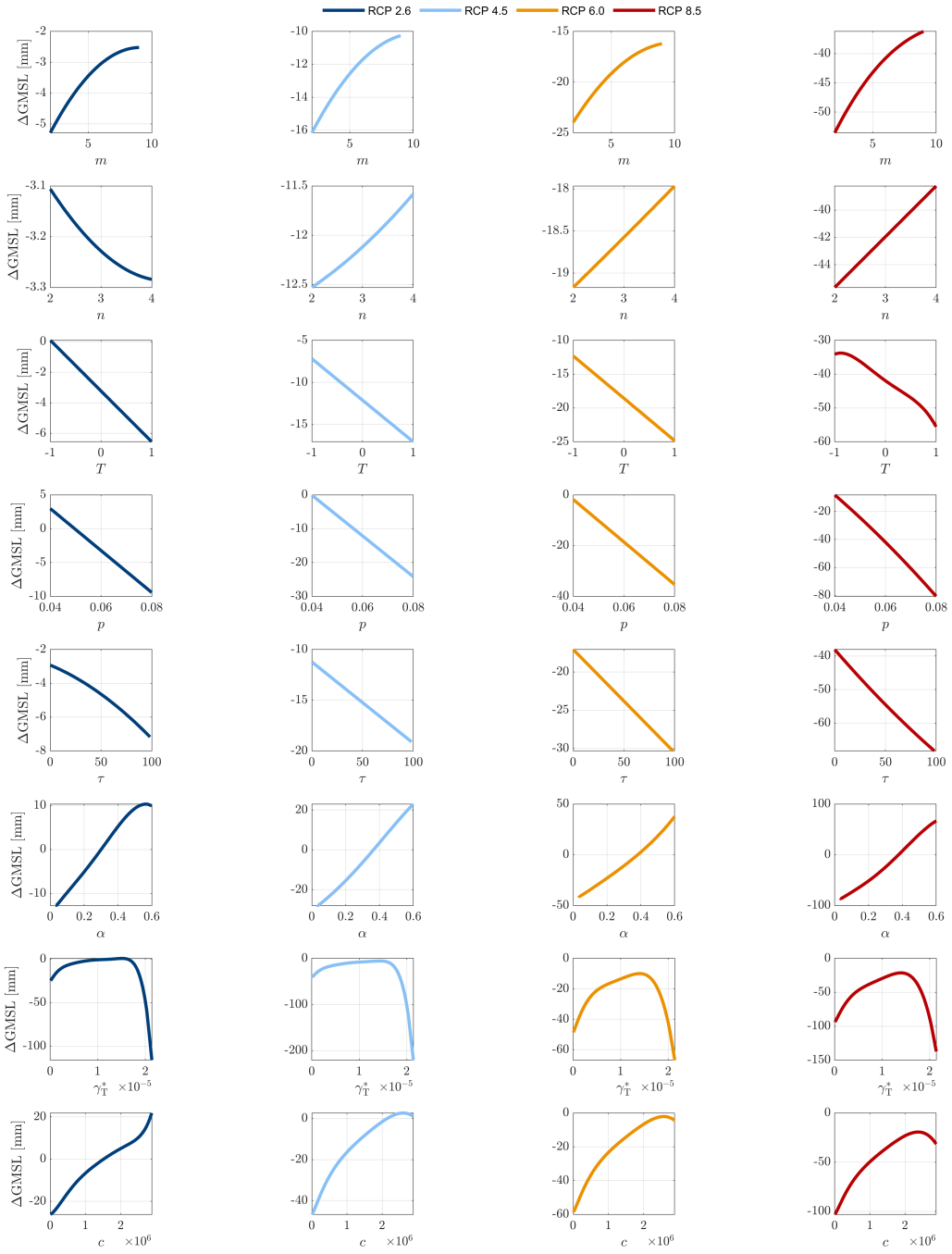

Figure S2. Individual parameter to projection (ΔGMSL) response for each parameter and RCP scenario. Each PCE model was re-evaluated for each parameter individually, while the remaining parameters were held at their point estimates (see Figure 3 in the main text)

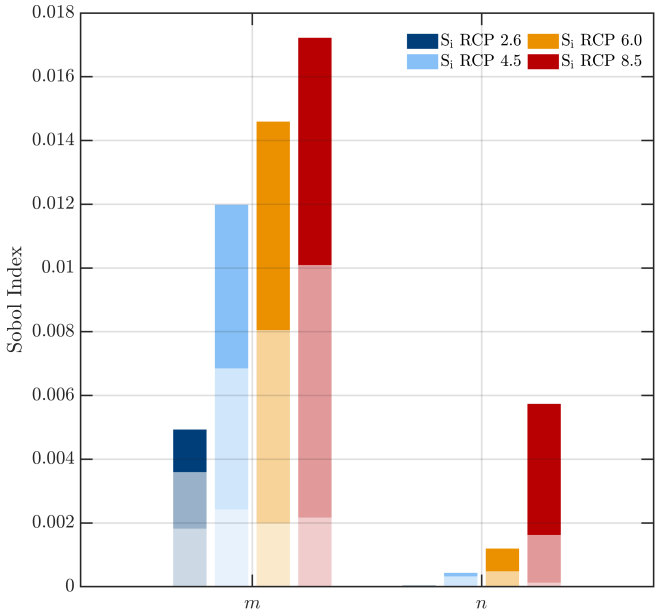

Figure S3. First order Sobol indices for m and n parameters only, for each RCP forcing scenario. Dark shading shows the Sobol indices for ΔGMSL in 2300. Two lighter shading colours represent Sobol indices at years 2100 and 2200, to show the variability in parameter importance through time.

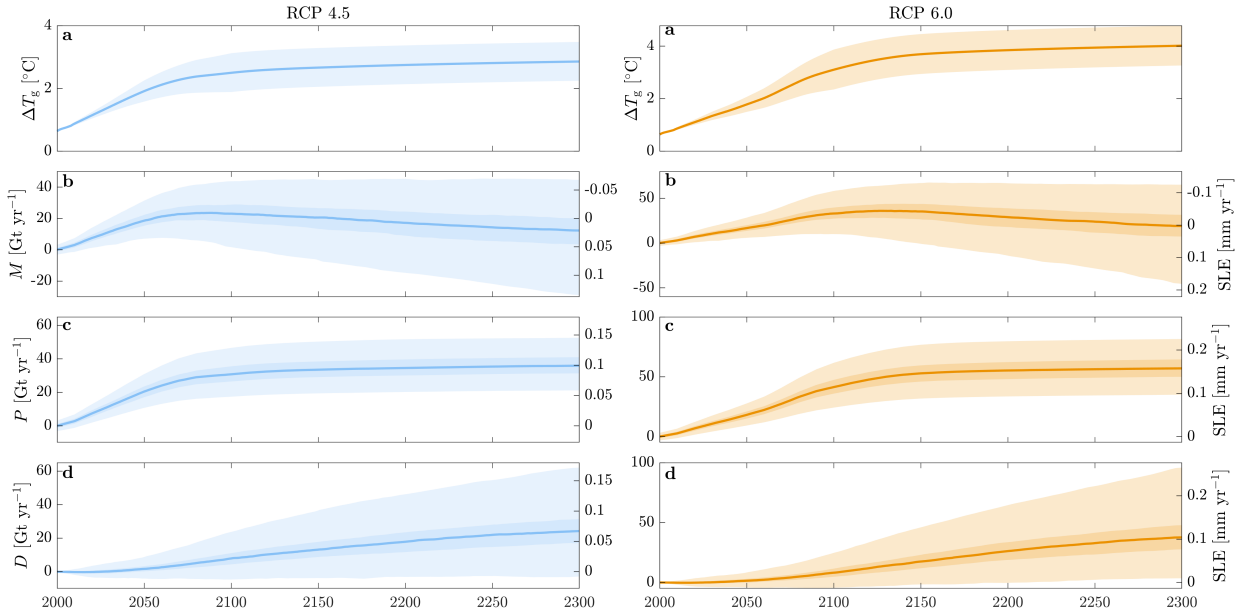

Figure S4. Projected temperature changes and mass balance changes for RCP 4.5 (left panels, blue lines) and RCP 6.0 (right, red) between 2000 and 2300 from our ensemble. Uncertainties are shown between 5 and 95% in light shading and between 33 and 66% in dark shading **a, e)** Global temperature anomalies, **b, f)** Change in the rate of total mass change (M) in Gt yr^{-1} calculated as $P - D$ **c, g)** Change in rate of accumulation integrated over the grounded area (P Gt yr^{-1}) with respect to our control runs ($P_{\mathrm{rcp}} - P_{\mathrm{ctrl}}$). **d, h)** Change in the rate of ice discharge integrated across the grounding line (D Gt yr^{-1}) calculated with respect to our control runs ($D_{\mathrm{rcp}} - D_{\mathrm{ctrl}}$)

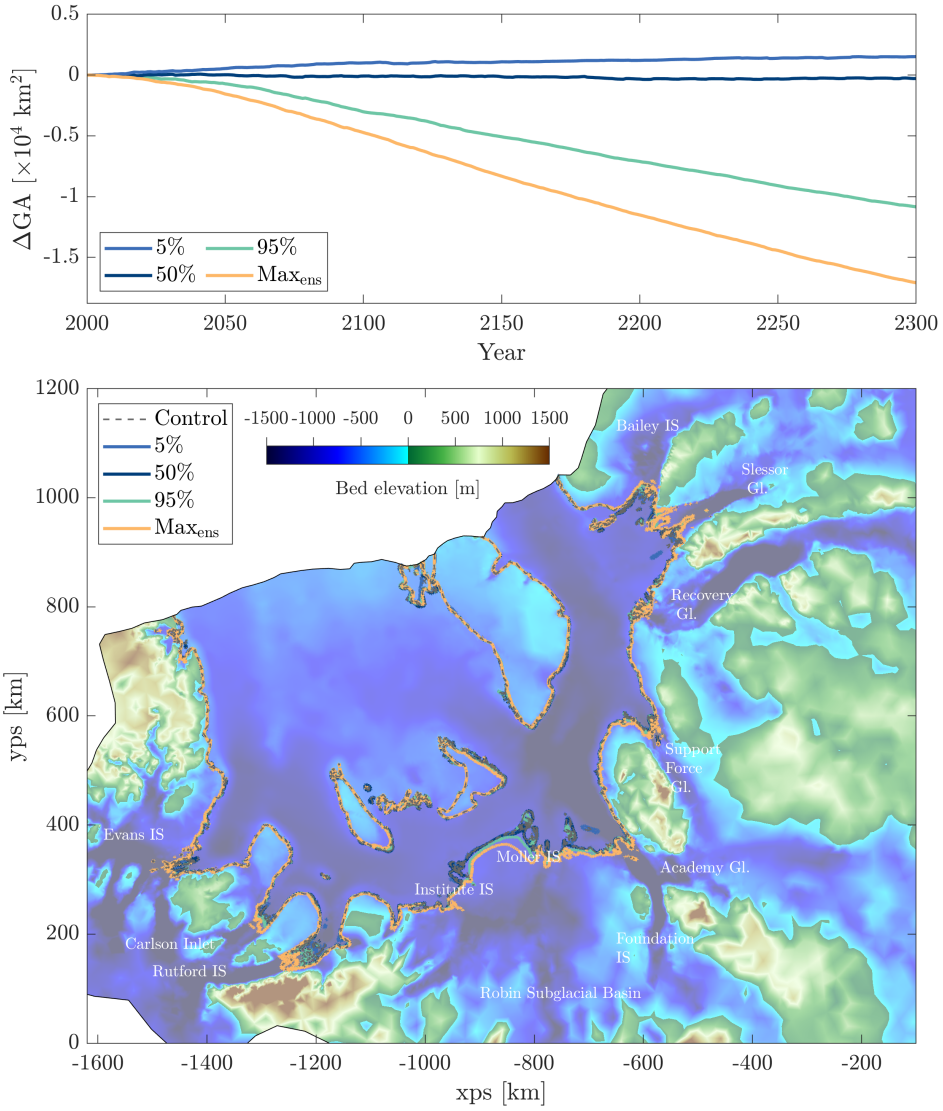

Figure S5. Changes in grounded area and grounding line position for RCP 2.6. Top panel shows change in grounded area (ΔGA calculated as $\mathrm{GA_{rcp}} - \mathrm{GA_{ctrl}}$) in $\times 10^4 \mathrm{km}^2$. Coloured lines represent the 5th, 50th and 95th percentiles of the projections of ΔGMSL rather than the percentiles of the change in grounded area itself. However, they are generally close to the grounded area results. Lower panel shows the FR basin and bed elevation above (green to brown) and below (light to dark blue) sea level. Coloured lines show grounding line positions from our ensemble simulations that lie closest to our percentiles (5, 50 and 95%) from our surrogate model projections, with respect to control runs (dashed grey lines). The grounding line position of the maximum ΔGMSL from our ensemble is also shown (orange).

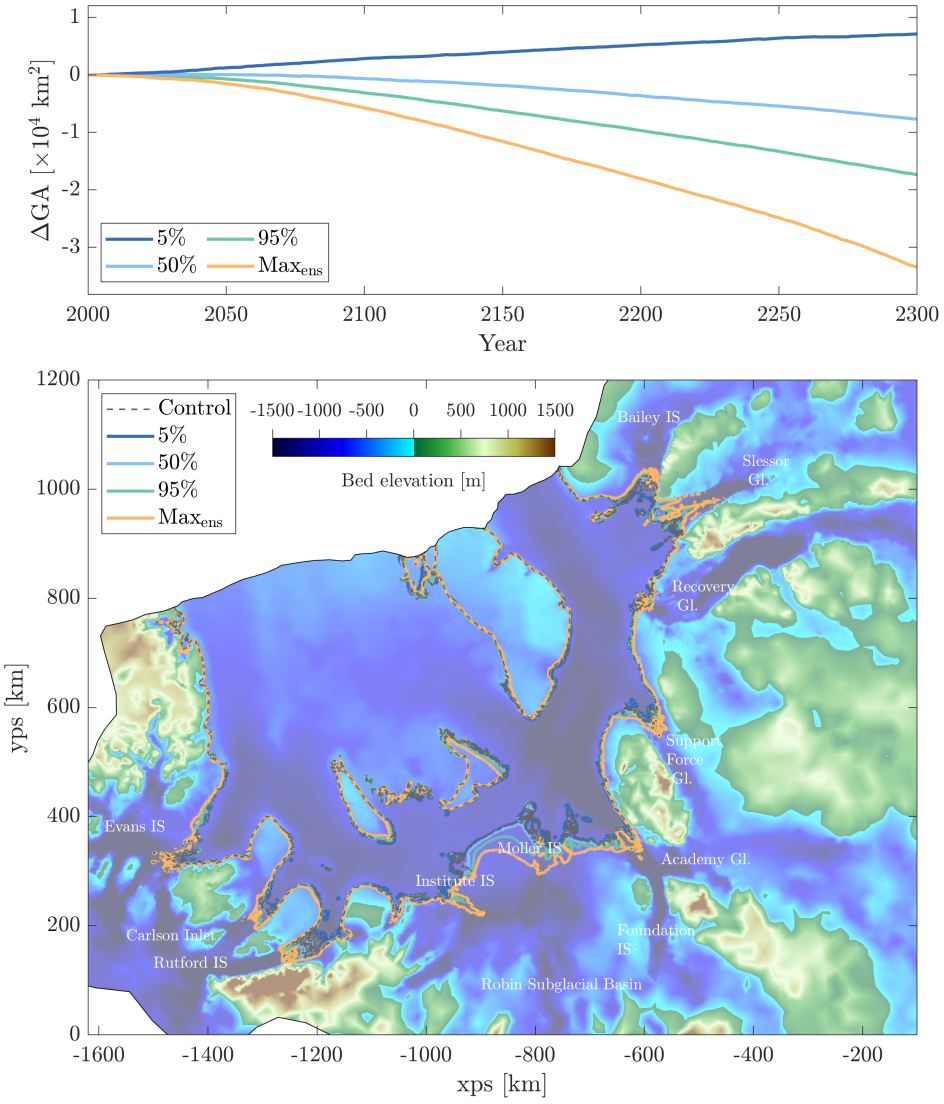

Figure S6. Changes in grounded area and grounding line position for RCP 4.5. Top panel shows change in grounded area (ΔGA calculated as $\mathrm{GA_{rcp}} - \mathrm{GA_{ctrl}}$) in $\times 10^4 \mathrm{km}^2$. Coloured lines represent the 5th, 50th and 95th percentiles of the projections of ΔGMSL rather than the percentiles of the change in grounded area itself. However, they are generally close to the grounded area results. Lower panel shows the FR basin and bed elevation above (green to brown) and below (light to dark blue) sea level. Coloured lines show grounding line positions from our ensemble simulations that lie closest to our percentiles (5, 50 and 95%) from our surrogate model projections, with respect to control runs (dashed grey lines). The grounding line position of the maximum ΔGMSL from our ensemble is also shown (orange).

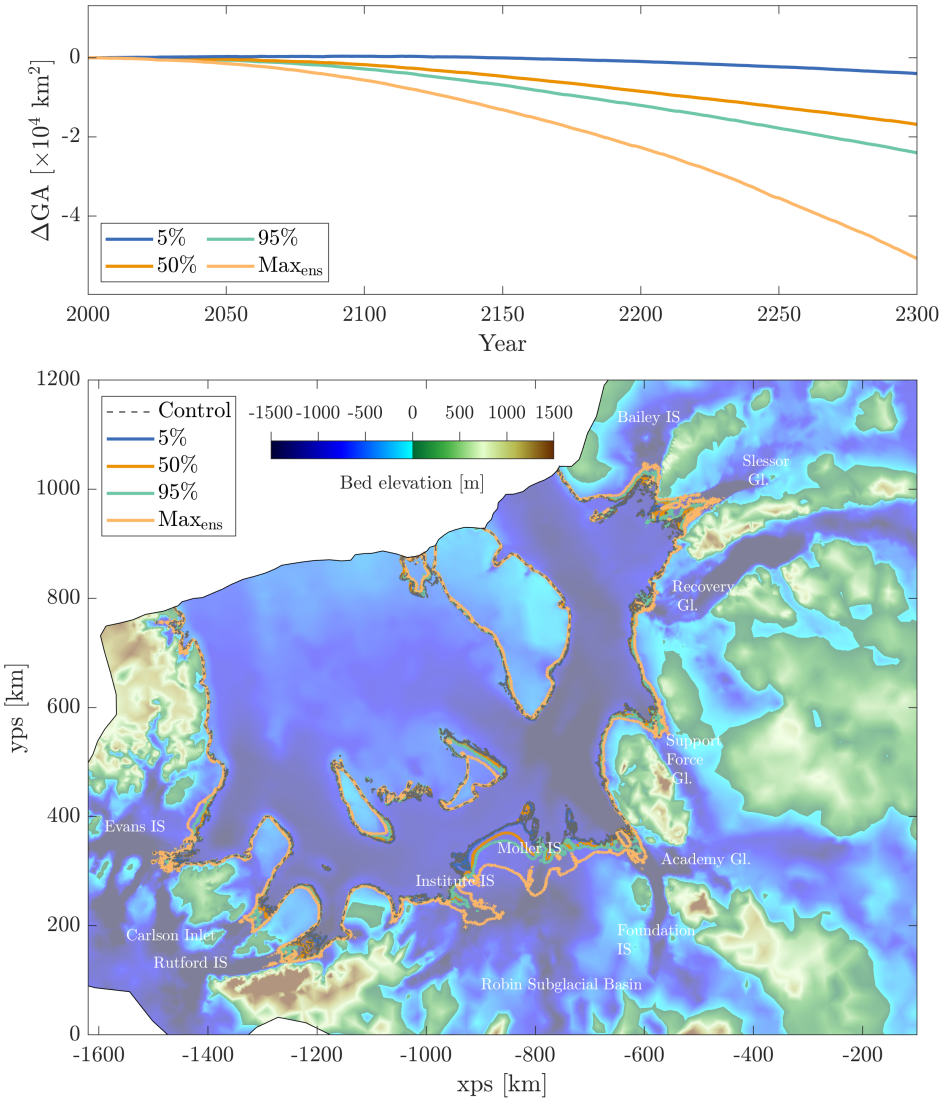

Figure S7. Changes in grounded area and grounding line position for RCP 6.0. Top panel shows change in grounded area (ΔGA calculated as $\mathrm{GA_{rcp}} - \mathrm{GA_{ctrl}}$) in $\times 10^4 \mathrm{km}^2$. Coloured lines represent the 5th, 50th and 95th percentiles of the projections of ΔGMSL rather than the percentiles of the change in grounded area itself. However, they are generally close to the grounded area results. Lower panel shows the FR basin and bed elevation above (green to brown) and below (light to dark blue) sea level. Coloured lines show grounding line positions from our ensemble simulations that lie closest to our percentiles (5, 50 and 95%) from our surrogate model projections, with respect to control runs (dashed grey lines). The grounding line position of the maximum ΔGMSL from our ensemble is also shown (orange).

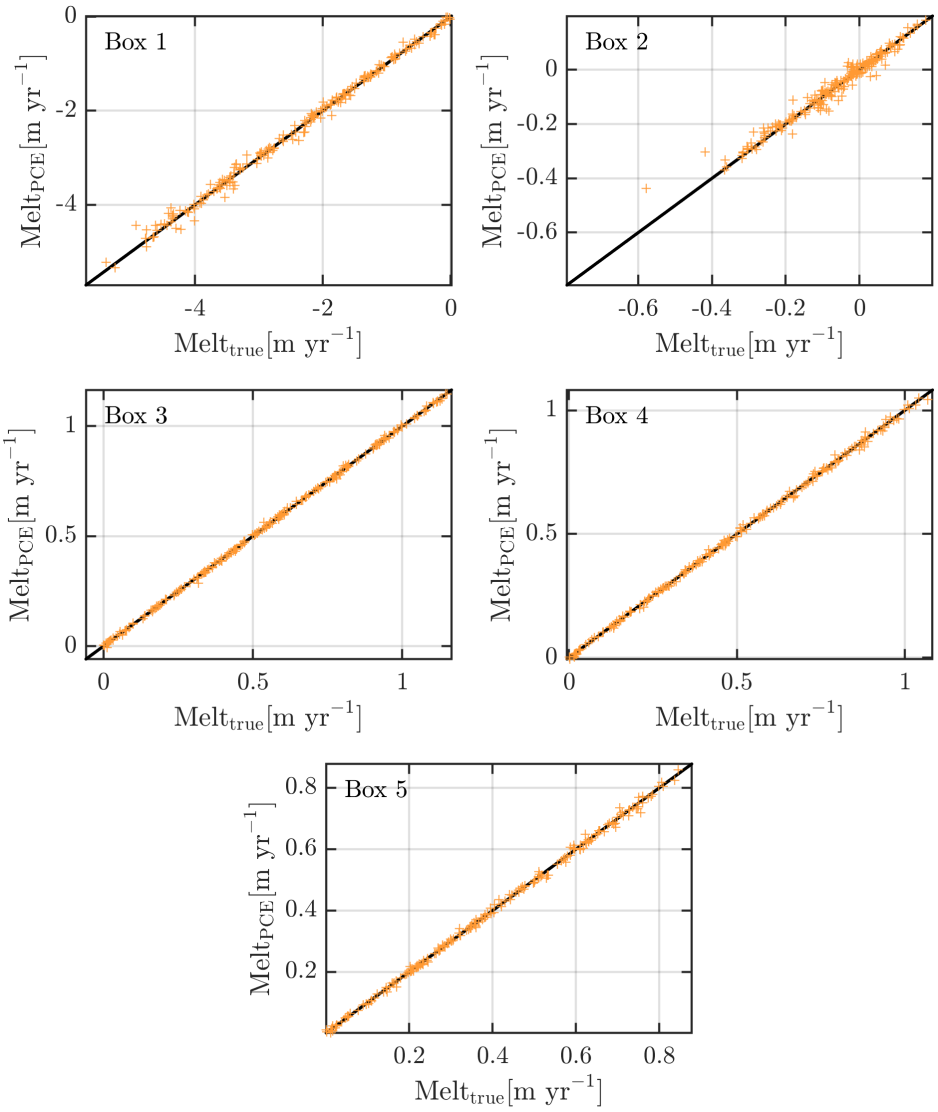

Figure S8. Performance of our surrogate (PCE) models used to simulate melting in each box of the ocean-box model. Values are the area-integrated ice-shelf melt rates in m yr^{-1} calculated directly in the ocean-box model (x-axis), and simulated by the PCE (y-axis).

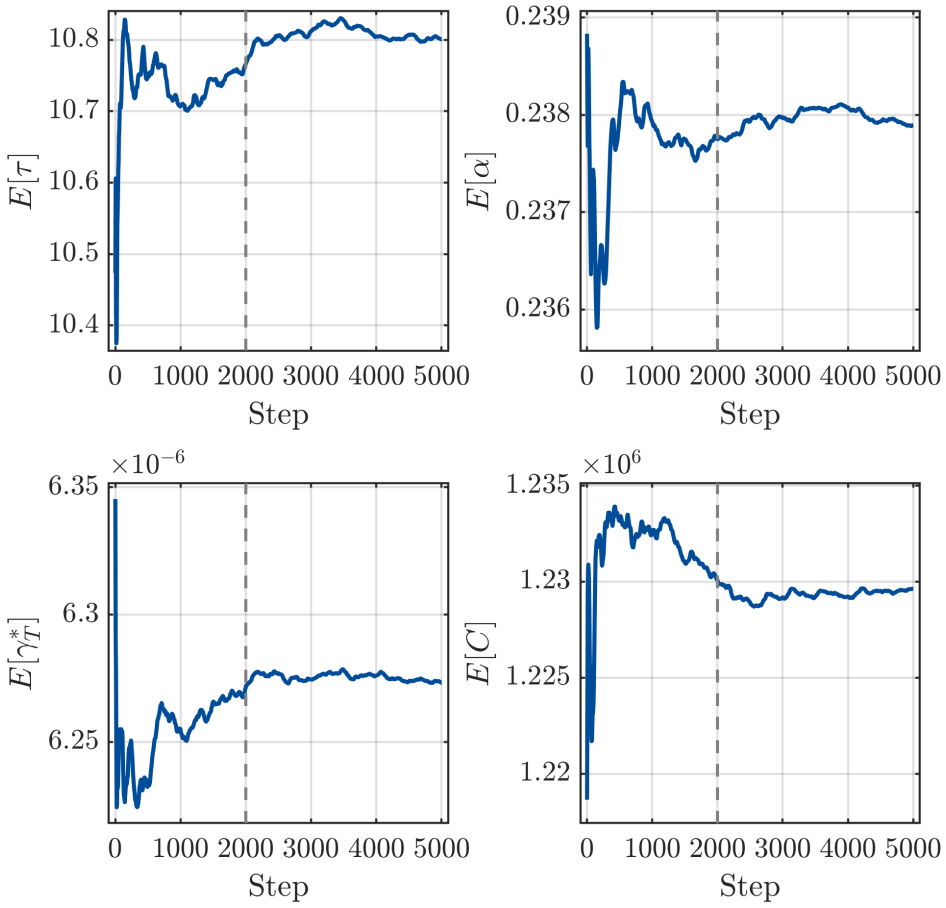

Figure S9. Convergence plot of the empirical mean for each hyperparameter averaged over all the Monte Carlo Markov chains to determine the number of sample points to discard (burn-in) that were generated prior to convergence. We discard the first 2000 points as burn-in.